

Differentiable Forward Kinematics for TensorFlow 2

Lukas Mölschl¹, Jakob Hollenstein², and Justus Piater³

Abstract—Robotic systems are often complex and depend on the integration of a large number of software components. One important component in robotic systems provides the calculation of *forward kinematics*, which is required by both motion-planning and perception related components. End-to-end learning systems based on deep learning require passing gradients across component boundaries.

Typical software implementations of forward kinematics are not differentiable, and thus prevent the construction of gradient-based, end-to-end learning systems.

In this paper we present a library compatible with *ROS-URDF* that computes forward kinematics while simultaneously giving access to the gradients w.r.t. joint configurations and model parameters, allowing gradient-based learning and model identification. Our Python library is based on TensorFlow 2 and is auto-differentiable. It supports calculating a large number of kinematic configurations on the GPU in parallel, yielding a considerable performance improvement compared to sequential CPU-based calculation.

<https://github.com/lumoe/dlkinematics.git>

I. INTRODUCTION

Adaptable, learning robots are an active topic of research. One promising approach for the realization of such robotic systems are end-to-end trainable systems. End-to-end trainable means that the software components of the system are able to adapt and to pass learning information across component boundaries. Deep-learning-based end-to-end trainable systems are typically optimized by gradient descent and the learning information consists of the gradients of a components outputs with respect to its inputs or parameters. Components that can provide the gradient information are called *differentiable*. Most robotic system component implementations are not differentiable and thus prevent the construction of end-to-end trainable systems.

Calculating the *forward kinematics*, the end-effector pose and all intermediate transformation matrices, is a necessary task in virtually all robotic systems. Although components to calculate forward-kinematics are typically provided by robotic frameworks, such as the Robot Operating System (ROS) [19], they are usually not differentiable.

An easy to use, differentiable forward kinematics implementation benefits a wide range of tasks. For example, James et al. [14] resort to learning the forward kinematics using

a deep neural network. They train a visuomotor control policy that outputs target positions based on the camera image and the robots joint positions. This architecture has to implicitly learn the forward kinematics and could instead benefit from an explicit forward kinematic component as proposed in this paper. Another example is the use of a kinematic model as an inductive bias: Zhou et al. [22] propose using a kinematic layer in vision-to-pose regressions and show improved performance for both, a toy robot arm example, as well as full-fledged human pose estimation. Villegas et al. [21] also found that the accuracy of pose estimation can be improved by the use of a kinematic layer. In contrast to explicitly building the forward-kinematic architecture for each kinematic model by adjusting the source code, our library provides a forward-kinematic layer based on the Universal Robot Description Format (URDF) description of the kinematic model and thus greatly simplifies the implementation. Calculating inverse kinematics is also often required and learning the inverse kinematic mapping has been explored [15], [7]. Even such learning approaches can benefit from a differentiable forward-kinematic component, for example by verifying the estimated inverse kinematics against a known-good forward-kinematic calculation or by refining a predicted inverse mapping: gradient-based local optimization of the forward kinematics can improve the accuracy of the predicted joint configuration.

In this paper we present *DLKinematics*, a building block for end-to-end deep learning in robotic projects. Our library allows batch computation of forward kinematics, greatly improving the computational efficiency as shown in our empirical analysis. The simplicity of our library—calculation of kinematic chains described in URDF files is possible with two lines of code—further unlocks the potential of deep learning techniques in robotics. To the best of our knowledge, we present the first Python library based on the widely used deep-learning package TensorFlow 2, that provides auto-differentiable forward kinematic calculations for kinematics described in the Universal Robot Description Format (URDF) popularized by ROS.

A. Related Work

Robotic software frameworks (e.g., ROS [19], *armarx* [20]) typically include components to describe kinematic chains and perform kinematic motion planning, e.g. KDL [12], MoveIT [6], [10], which are not differentiable. This means they do not provide the gradient information of their outputs with respect to their inputs or parameters. This restriction impedes a straightforward application of gradient-based learning techniques.

¹Lukas Mölschl is a student in Faculty of Informatics at the TU Wien, Erzherzog-Johann-Platz 1 1040 Vienna, Austria lukas@moelschl.com

²Jakob Hollenstein is with the Department of Computer Science, University of Innsbruck, Technikerstraße 21a, 6020 Innsbruck, Austria jakob.hollenstein@uibk.ac.at

³Justus Piater is with the Department of Computer Science, University of Innsbruck, Technikerstraße 21a, 6020 Innsbruck, Austria justus.piater@uibk.ac.at

The difficulty of writing differentiable components for end-to-end learning has been drastically reduced by the advent and subsequent wide availability of auto-differentiation libraries, most prominently for Python [2], [4], [18] but also for languages more traditionally associated with robotics such as C++ [3].

The availability of automatic differentiation libraries reduces the barrier to entry and blurs the line between traditional approaches and deep-learning. For example, Ledezma et al. [16], [8] proposed the *first-order-principle networks*, that combine first-order engineering principles with deep-learning models to calculate robot dynamics. In a similar fashion Meier et al. [17] published a robot-dynamics component that seamlessly integrates with `pytorch`, while Carpentier et al. [5] propose a forward- and inverse-dynamics library written in C++. Beyond these methods are the full-fledged differentiable simulation libraries `brax` [9], and `TDS` [11]. While the former is written in `jax` and thus seamlessly integrates into the `jax` and `TensorFlow` frameworks, the latter provides similar capabilities but does not integrate into the Python learning systems. Both of these libraries are full-fledged simulators including simulation of contact dynamics but they are not tailored to extract the forward kinematics. The component by Meier et al. [17] is the closest substitute for calculating the forward kinematics in `pytorch`, while our component is built for `TensorFlow`. The benefits of our component are the ease of use and integration for calculating forward-kinematics from arbitrary URDF models in `TensorFlow`.

II. METHOD

Positions and *orientations* in 3D space are defined relative to a reference frame, the base frame, where $(x, y, z) \in \mathbb{R}^3$ defines the translations relative to the reference frame and $(\alpha, \beta, \gamma) \in \mathbb{R}^3$ define the rotations around (x, y, z) relative to the orientation of the reference frame. The combination $(x, y, z, \alpha, \beta, \gamma)$ of position and orientation is called a *pose* and consists of the translation and the angles describing the rotation. Each pose can define its own frame of reference, where the pose would be expressed as the zero pose $(0, 0, 0, 0, 0, 0)$. Thus a pose can be expressed as the *transformation* of the zero pose to or from a different reference frame. In this paper we express coordinates as homogeneous coordinates:

$$\begin{bmatrix} x & y & z \end{bmatrix}^T \rightarrow \begin{bmatrix} x & y & z & 1 \end{bmatrix}^T \quad (1)$$

This allows us to express transformations $\mathbf{T}_{i:j}$ between two reference frames i and j as a (4×4) matrix, consisting of a (3×3) rotation matrix $\mathbf{R}_{i:j}$ and a (3×1) translation matrix $\mathbf{P}_{i:j}$:

$$\mathbf{T}_{i:j} = \begin{bmatrix} \mathbf{R}_{i:j} & \mathbf{P}_{i:j} \\ 0 & 1 \end{bmatrix} \quad (2)$$

The rotation matrix $\mathbf{R}_{i:j}$ is constructed from rotations

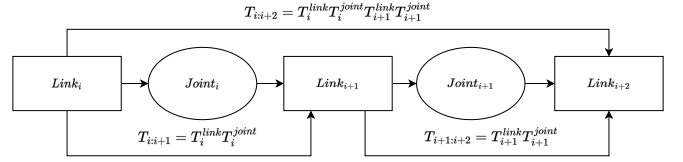


Fig. 1: Transformations between link_n to link_{n+2} visualized

around each axis.

$$\mathbf{R}_{i:j} = \mathbf{R}_{z,i:j}(\gamma_{i:j}) \mathbf{R}_{y,i:j}(\beta_{i:j}) \mathbf{R}_{x,i:j}(\alpha_{i:j}) \quad (3)$$

$$\mathbf{R}_{x,i:j}(\alpha_{i:j}) = \begin{bmatrix} 1 & 0 & 0 \\ 0 & \cos \alpha_{i:j} & -\sin \alpha_{i:j} \\ 1 & \sin \alpha_{i:j} & \cos \alpha_{i:j} \end{bmatrix} \quad (4)$$

$$\mathbf{R}_{y,i:j}(\beta_{i:j}) = \begin{bmatrix} \cos \beta_{i:j} & 0 & \sin \beta_{i:j} \\ 0 & 1 & 0 \\ -\sin(\beta_{i:j}) & 0 & \cos \beta_{i:j} \end{bmatrix} \quad (5)$$

$$\mathbf{R}_{z,i:j}(\gamma_{i:j}) = \begin{bmatrix} \cos \gamma_{i:j} & -\sin \gamma_{i:j} & 0 \\ \sin \gamma_{i:j} & \cos \gamma_{i:j} & 0 \\ 0 & 0 & 1 \end{bmatrix} \quad (6)$$

The result is a single rotation matrix with order z, y, x shown below. For brevity we denote $\cos(\alpha_{i:j})$ by $c_{\alpha_{i:j}}$ and $\sin(\alpha_{i:j})$ by $s_{\alpha_{i:j}}$. $\mathbf{R}_{i:j}$:

$$\begin{bmatrix} c_{\alpha_{i,j}} c_{\gamma_{i,j}} & -c_{\alpha_{i,j}} s_{\gamma_{i,j}} + c_{\gamma_{i,j}} s_{\alpha_{i,j}} s_{\beta_{i,j}} & c_{\alpha_{i,j}} c_{\gamma_{i,j}} s_{\beta_{i,j}} + s_{\alpha_{i,j}} s_{\gamma_{i,j}} \\ c_{\beta_{i,j}} s_{\gamma_{i,j}} & c_{\alpha_{i,j}} c_{\gamma_{i,j}} + s_{\alpha_{i,j}} s_{\beta_{i,j}} s_{\gamma_{i,j}} & c_{\alpha_{i,j}} s_{\beta_{i,j}} s_{\gamma_{i,j}} - c_{\gamma_{i,j}} s_{\alpha_{i,j}} \\ s_{\gamma_{i,j}} & c_{\beta_{i,j}} s_{\alpha_{i,j}} & c_{\alpha_{i,j}} c_{\beta_{i,j}} \end{bmatrix} \quad (7)$$

Given multiple transformations $\mathbf{T}_{i:i+1}, \dots, \mathbf{T}_{j-1:j}$, a combined transformation $\mathbf{T}_{i:j}$ is calculated by:

$$\mathbf{T}_{i:j} = \mathbf{T}_{i:i+1} \mathbf{T}_{i+1:i+2} \dots \mathbf{T}_{j-2:j-1} \mathbf{T}_{j-1:j} \quad (8)$$

In this paper we describe the kinematics of a robot as a tree consisting of links (static) and joints (moveable). Each node in the tree defines a reference frame, for example the frame at the end of a link, or the frame describing the displacement or rotation due to a joint. Two links are always connected by a joint (Fig. 1).

A *kinematic chain* describes a sub-path between nodes in this tree, e.g. link_i ... link_j. Using the transformations along the path $\mathbf{T}_{i:i+1}, \dots, \mathbf{T}_{j-1:j}$, the complete transformation $\mathbf{T}_{i:j}$ from link_i to link_j is calculated. For example, in a robot with two end-effectors, the two transformations between the robot base and each of the end-effectors are described by two separate kinematic chains.

A. Implementation Details

1) *Unified Robot Description Format (URDF)*: URDF is a standardized XML file format used to describe the kinematic properties of a robot, i.e. its joints and links. The URDF [1] specifies different types of joints: revolute (hinge), continuous (continuous hinge), prismatic (sliding), fixed, planar and floating (6-DoF joint). The most generic joint is the 6-DoF joint (floating) joint. According to the URDF specifications, a constraint exists wherein each joint

must have exactly one parent link and child link. It is not possible for a joint to be followed by another joint or for a link to be followed by another link. The URDF defines the kinematic structure as a tree with parent-child relationships and defines relative translations and rotations. Joint properties such as limits can be specified. For further details refer to [1].

2) *Modelling by 6-DoF joint*: The 6-DoF joint fully parameterizes a (4×4) homogeneous transformation matrix. The 6-DoF joint is parameterized by six parameters in the form $[x, y, z, \alpha, \beta, \gamma]$ where $[x, y, z]$ represent translation and $[\alpha, \beta, \gamma]$ describes rotation around each axis. All other joint types can be derived from this joint by fixing all but the relevant axes. For example, a prismatic joint, with one degree of freedom, that can slide along the y axis, can be represented as a 6-DoF joint in the form $[0, y, 0, 0, 0, 0]$. A revolute joint, with one degree of freedom, that rotates around the z axis, would be parameterized by γ in the form $[0, 0, 0, 0, 0, \gamma]$. This structure is used to model all joint types defined in the URDF specifications.

3) *Vectorized Implementation*: Let a kinematic chain of interest be denoted by $\mathbf{T}_{0:1}^L, \mathbf{T}_{0:1}^J \dots \mathbf{T}_{n-1:n}^L \mathbf{T}_{n-1:n}^J$, and $\mathbf{T}_{0:n}$ denotes the complete transformation from the initial frame to the end of the kinematic chain, e.g. the end-effector. The transformation $\mathbf{T}_{0:n}$ is composed alternately of two components: a transformation along a link \mathbf{T}_{ii+1}^L , and a transformation along a joint \mathbf{T}_{ii+1}^J . Since the parameters of the links are static, \mathbf{T}_{ii+1}^L are pre-computed during the initialization phase according to the URDF, while \mathbf{T}_{ii+1}^J are parameterized.

Let b denote the batch-size, i.e. the number of different joint configurations for which the forward kinematic calculations are performed, and n denotes the number of joints.

The dynamic transformations \mathbf{T}_{ii+1}^J along the joints are calculated by partially parameterizing 6-DoF joints. These parameterizations are stored in a $(b \times n \times 6)$ tensor \mathbf{Q} :

$$\mathbf{Q} = \begin{bmatrix} \begin{bmatrix} x_{0:1}^{(1)} & y_{0:1}^{(1)} & z_{0:1}^{(1)} & \alpha_{0:1}^{(1)} & \beta_{0:1}^{(1)} & \gamma_{0:1}^{(1)} \\ \vdots & \vdots & \vdots & \vdots & \vdots & \vdots \\ x_{n-1:n}^{(1)} & y_{n-1:n}^{(1)} & z_{n-1:n}^{(1)} & \alpha_{n-1:n}^{(1)} & \beta_{n-1:n}^{(1)} & \gamma_{n-1:n}^{(1)} \end{bmatrix} \\ \vdots \\ \begin{bmatrix} x_{0:1}^{(b)} & y_{0:1}^{(b)} & z_{0:1}^{(b)} & \alpha_{0:1}^{(b)} & \beta_{0:1}^{(b)} & \gamma_{0:1}^{(b)} \\ \vdots & \vdots & \vdots & \vdots & \vdots & \vdots \\ x_{n-1:n}^{(b)} & y_{n-1:n}^{(b)} & z_{n-1:n}^{(b)} & \alpha_{n-1:n}^{(b)} & \beta_{n-1:n}^{(b)} & \gamma_{n-1:n}^{(b)} \end{bmatrix} \end{bmatrix} \quad (9)$$

The parameterization of the degrees of freedom $\theta_1^{(k)}, \dots, \theta_m^{(k)}$ are modelled, following the explanation in Sec. II-A.2 by modifying the corresponding parameters in \mathbf{Q} . How to map from $\theta_i^{(k)}$ to parameters of \mathbf{Q} is determined by indexing. The batch of joint configurations, Θ is a $(bm \times 1)$ matrix:

$$\Theta = [\theta_1^{(1)} \quad \dots \quad \theta_m^{(1)} \quad \dots \quad \theta_1^{(b)} \quad \dots \quad \theta_m^{(b)} \quad \dots]^\top \quad (10)$$

The index matrix \mathbf{P} , is a $(bm \times 3)$ matrix:

$$\mathbf{P} = \begin{bmatrix} c_1^{(1)} & d_1^{(1)} & e_1^{(1)} \\ \vdots & \vdots & \vdots \\ c_m^{(1)} & d_m^{(1)} & e_m^{(1)} \\ \vdots & \vdots & \vdots \\ c_1^{(b)} & d_1^{(b)} & e_1^{(b)} \\ \vdots & \vdots & \vdots \\ c_m^{(b)} & d_m^{(b)} & e_m^{(b)} \end{bmatrix} \quad (11)$$

$c_j^{(i)}$ is set to i and maps $\theta_j^{(i)}$ to the i -th batch in \mathbf{Q} . $d_j^{(i)} \in \{1, \dots, n\}$ denotes the row of the i -th batch in \mathbf{Q} . $e_j^{(i)}$ denotes the target parameter $\{1, \dots, 6\} \mapsto \{x, \dots, \gamma\}$. These indices are only calculated during the first call, allowing for sparse updates to the zero matrix during the forward call and the incorporation of dynamic joint configurations into the matrix. Mapping from Θ to \mathbf{Q} is efficiently implemented using `scatter_nd` and is executed on the GPU.

For all 6-DoF joint configurations specified in \mathbf{Q} the associated transformation matrices $\mathbf{T}_{i:j}^{J(k)}$ are calculated in parallel, yielding a $(b \times n \times 4 \times 4)$ tensor, \mathfrak{T}^J .

$$\mathfrak{T}^J = \begin{bmatrix} \begin{bmatrix} \mathbf{T}_{0:1}^{J(1)} \\ \vdots \\ \mathbf{T}_{0:1}^{J(b)} \end{bmatrix} & \dots & \begin{bmatrix} \mathbf{T}_{n-1:n}^{J(1)} \\ \vdots \\ \mathbf{T}_{n-1:n}^{J(b)} \end{bmatrix} \end{bmatrix} \quad (12)$$

The pre-computed static transformations \mathbf{T}_{i+j}^L are stored as a $(b \times n \times 4 \times 4)$ tensor \mathfrak{T}^L (links):

$$\mathfrak{T}^L = \begin{bmatrix} \begin{bmatrix} \mathbf{T}_{0:1}^{L(1)} \\ \vdots \\ \mathbf{T}_{0:1}^{L(b)} \end{bmatrix} & \dots & \begin{bmatrix} \mathbf{T}_{n-1:n}^{L(1)} \\ \vdots \\ \mathbf{T}_{n-1:n}^{L(b)} \end{bmatrix} \end{bmatrix} \quad (13)$$

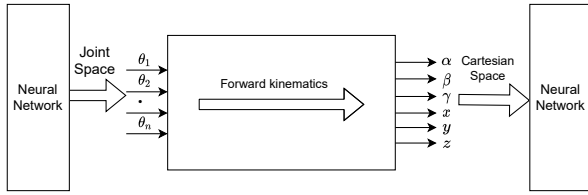
A combined transformation \mathfrak{T}^{LJ} is calculated by combining all k, i : $\mathbf{T}_{i:i+1}^{LJ(k)} = \mathbf{T}_{i:i+1}^{L(k)} \mathbf{T}_{i:i+1}^{J(k)}$. This operation is efficiently parallelized across the batch dimension $k \in \{1, \dots, b\}$ and link-joint segment $i \in \{1, \dots, n\}$.

Following (7), efficiently implemented using a `scan` operation, the b kinematic chains of transformations of \mathfrak{T}^{LJ} are sequentially combined into complete forward transformations \mathfrak{T}' :

$$\mathfrak{T}' = \begin{bmatrix} \begin{bmatrix} \mathbf{T}_{0:1}^{LJ(1)} \\ \vdots \\ \mathbf{T}_{0:1}^{LJ(b)} \end{bmatrix} & \dots & \begin{bmatrix} \mathbf{T}_{0:n}^{LJ(1)} \\ \vdots \\ \mathbf{T}_{0:n}^{LJ(b)} \end{bmatrix} \end{bmatrix} \quad (14)$$

Depending on the use case \mathfrak{T}' or simple the final transformations are returned, i.e. $(b \times 4 \times 4)$:

$$\begin{bmatrix} \mathbf{T}_{0:n}^{LJ(1)} & \dots & \mathbf{T}_{0:n}^{LJ(b)} \end{bmatrix} \quad (15)$$



(a) The Forward Kinematics calculation can be used as a building block in any algorithm but can also easily be embedded as a neural network layer.

```

from dlkinematics.training_utils import
    ForwardKinematics

model = keras.Sequential()

FK_layer = ForwardKinematics(
    urdf_file = 'path/to/urdf',
    base_link = 'link0',
    end_link = 'linkN',
    batch_size = 32)

# model.add(... NN layers ...)
model.add(FK_layer)
# model.add(... NN layers ...)

```

(b) Embedding the calculation as a layer requires two lines of code.

Fig. 2: Example of embedding FK calculations for a URDF file as a neural network layer.

III. LIBRARY USAGE EXAMPLES

A. Embedding Forward Kinematics in a Neural Network

Keras is a high-level API for TensorFlow. It allows users to easily define and train deep neural networks by specifying the network in terms of layers, thereby abstracting the underlying workings of TensorFlow.

`DLKinematics` integrates into this ecosystem by providing a class that can be added as a Keras layer, illustrated in Fig. 2a. Creating such a forward kinematics layer and embedding it into a Keras model requires just two lines of code as in Fig. 2b. In such a setup, the network would calculate joint configurations, e.g., based on an image, and the forward kinematics layer would output the pose. This pose can be used as part of the loss function or be further processed by additional neural-network layers.

B. Calculating Jacobian Matrix

A typical requirement in robotics is to calculate the Jacobian of the end-effector pose with respect to the joints, which is typically used to capture the relationship between joint velocities and the end-effector velocities.

The computation of the Jacobian matrix with `DLKinematics` is straightforward, as depicted in Fig. 3. In this listing, the forward kinematics for a batch of joint configurations and the resulting Jacobian matrix of the position and rotation of the end-effector with respect to the joint configuration are computed.

```

import tensorflow as tf
from dlkinematics.urdf import chain_from_urdf_file
from dlkinematics.dlkinematics import DLKinematics
from dlkinematics.tf_transformations import
    pose_from_matrix

# Load URDF
chain = chain_from_urdf_file('data/human.urdf')

# Create DLKinematics
dlkinematics = DLKinematics(
    chain,
    base_link="link0",
    end_link="link3",
    batch_size=2)

# Joint configuration
thetas = tf.convert_to_tensor([[1., 2., 3.], [3., 4.,
    6.]], dtype=tf.float32)

# Forward pass
with tf.GradientTape(persistent=True) as tape:
    tape.watch(thetas)
    fk_res = dlkinematics.forward(tf.reshape(thetas, (-1,
    )))
    p = pose_from_matrix(fk_res)

jacobian = tape.batch_jacobian(p, thetas)

```

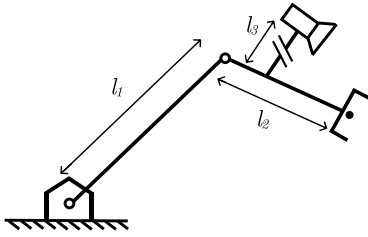
Fig. 3: Example of computing the Jacobian for a batch of simple joint configurations.

C. Kinematic Model Identification

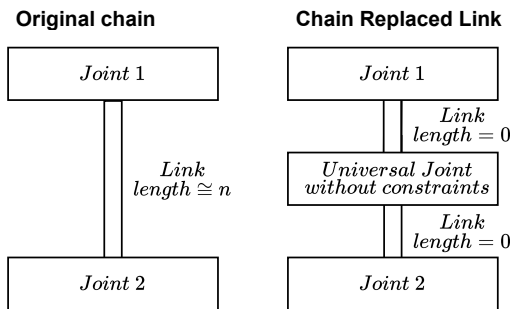
The kinematics description of robots and its physical realization might differ due to inaccuracies in production or the setup of the robot, for example the placement of cameras acting as visual sensors. An example of this is illustrated in Fig. 4a, where the link describing the camera position with respect to the end-effector is unknown or inaccurate. One way to overcome such a problem could be to record the location of the end-effector of a physical robot for a set of joint configurations. This data can then be used to compute the error between the estimated and expected location of the end-effector. In the next step our library can easily be used to iteratively estimate the real length and orientation of the links. We achieve this by replacing a link with a 6-DoF joint that gets initialized with the parameters of the original link from the URDF file (see Fig. 4b). A 6-DoF joint has six degrees of freedom and is therefore not bound to the original translation and orientation of the link. Using a gradient-based algorithm, estimate all six parameters of the 6-DoF joint. In addition to that, the `DLKinematics` provides functions to replace links with a 6-DoF joint (Fig. 4c). In an experiment with a chain of length four, we were able to estimate all six parameters of a link using gradient descent. Using a single fixed joint configuration and providing no prior estimate of the link, i.e. initializing the translation and rotation to zero, the algorithm converged in under 30 seconds (under 3000 gradient steps) with an accuracy in the range of 10^{-4} for each axis.

IV. EXPERIMENT: BATCH PROCESSING

In the process of training deep neural networks, samples are usually passed through the network in batches. By utilizing parallel processing wherever realizable, it is possible



(a) Kinematic model identification: The length and orientation of l_3 is unknown or inaccurate with respect to the end-effector and needs to be estimated.



(b) DLKinematics provides a function that replaces a link with a joint with six degrees of freedom

```

from dlkinematics.dlkinematics import DLKinematics
from dlkinematics.training_utils import
substitute_link_with_joint
from evaluation.estimate_model_params import
ParamEstimator
from evaluation.generate_dataset import Generator

# Loading kinematic chain ..

# Replace link with 6-DoF joint
new_chain = substitute_link_with_joint(urdf=dl_kin.
urdf,
target_link=target_link,root=root, last=last
)
dl_kin_new = DLKinematics(new_chain, root, last,
batch_size=batch_size)

sample_generator = Generator(urdf_file=path_to_urdf,
root_link=root, end_link=last, batch_size=
batch_size)

estimator = ParamEstimator(dl_kin, dl_kin_new,
batch_size=batch_size)

# Optimization loop
for idx, q_sample in enumerate(sample_generator.
joint_samples()):
res, iterations = estimator.step(q_sample.
flatten())
if np.mod(idx, num_samples) == 0:
break

print(f' {np.round(estimator.qs.numpy(), 3)}')
```

(c)

Fig. 4: Example of identifying link parameters through an optimization method.

to simultaneously compute the forward kinematics for a large number of joint configurations. This ability is crucial for population-based search methods, which are used, for example, in trajectory optimization. In this experiment, we use a kinematic chain with four degrees of freedom and measure the amount of forward kinematic computations per second. This is done using the comparison ground-truth library, `pykdl` on CPU, and our implementation on both CPU (AMD Ryzen 5 3600 6-Core) as well as GPU (NVIDIA GeForce RTX 3060 Ti). Note that `pykdl`, does not support parallel calculations. The experiment results on commodity hardware are shown in Table I. Our empirical evaluation shows that for a batch size of one, the additional call overhead is dominant, our implementation already achieves a much higher throughput at 256 parallel computations on both, the CPU and the GPU.

V. SUMMARY AND OUTLOOK

In this paper we present a differentiable forward kinematic library for kinematic representations described in the ROS

Batch Size	1	256	1024	4096
<code>pykdl</code> [ops/s]	20,010	-	-	-
DLKinematics CPU [ops/s]	485	91,980	202,819	374,491
DLKinematics GPU [ops/s]	537	114,551	338,773	802,318

TABLE I: Batch processing: Speedup in parallelization.

URDF format. Our library is built on and seamlessly integrates with `TensorFlow` and can be used as a building block in end-to-end learning systems in just three lines of code. We highlight the simplicity of embedding the forward kinematic calculation as a layer in `Keras` models as well as embedding it in `TensorFlow` calculations in general, show how to calculate end-effector jacobians and use it to identify and optimize unknown or inaccurate kinematic descriptions.

We benchmark our forward kinematic calculation library on a four degree of freedom kinematic chain, on both CPU and GPU, comparing the results with `pykdl`, a CPU-based library. We find that large batch computations suffer less from the call overhead associated with `TensorFlow` calculations. However, the number of forward-kinematic-calculations per second of our implementation largely outperforms the `pykdl` CPU-based library (using batched calculations with a batch size of 1024 configurations). The simplicity of our module, combined with its computational efficiency, unravels the application of modern deep learning techniques to robotics, and the inclusion of forward kinematics in end-to-end learning.

VI. APPENDIX

A. Rotation Distance Functions

Determining the error between the expected and actual output of a model is a task often required in machine learning systems. For the translation it is sufficient to use

```

from dlkinematics.training_utils import phi5_loss

result = dlkinematics.forward([1., 2., 3.])
# target ... transformation matrix [batch size, 4, 4]
error = phi5_loss(result, target)

```

Fig. 5: Example use of the rotational-distance metric Φ_5 .

the Euclidean distance. However, rotation matrices require different metrics.

DLKinematics therefore implements five different distance functions from [13] to compute metrics for the difference between two rotation matrices. All functions allow batch processing of $[batch_size \times 4 \times 4]$ homogeneous transformation matrices. The five functions Φ_1 , Φ_2 , Φ_3 , Φ_4 , Φ_5 are briefly described with respect to their calculation, signature, function name and an example usage is shown in Fig 5:

Euclidean distance of Euler angles `rotation_with_rmse`
Computing the Euclidean distance between two Euler angles,

$$\Phi_1 = \sqrt{(\alpha - \hat{\alpha})^2 + (\beta - \hat{\beta})^2 + (\gamma - \hat{\gamma})^2}.$$

The function internally extracts the Euler angles from the matrix. Signature: $T_1 \times T_2 \rightarrow \mathbb{R}^+$.

Euclidean distance between two quaternions `phi2_loss`
Computing the Euclidean distance between two quaternions, $\Phi_2 = \min\{\|q - \hat{q}\|, \|q + \hat{q}\|\}$. The function internally extracts quaternions from the matrix. Signature: $T_1 \times T_2 \rightarrow \mathbb{R}^+ \in [0, \sqrt{2}]$.

Inner products between two quaternions `phi3_loss`
Computing the inner product of two quaternions. $\Phi_3 = \arccos(|q - \hat{q}|)$ The function internally extracts quaternions from the matrix. Signature: $T_1 \times T_2 \rightarrow \mathbb{R}^+ \in [0, \pi/2]$.

Absolute quaternion inner product `phi4_loss`
Similar to `phi3_loss`, except that the inverse cosine function is replaced, $\Phi_4 = 1 - (|q - \hat{q}|)$. The function internally extracts quaternions from the matrix. Signature: $T_1 \times T_2 \rightarrow \mathbb{R}^+ \in [0, 1]$.

Deviation from the identity matrix `phi5_loss`
Computes the deviation from the identity matrix, $\Phi_5 = \|\mathbf{I} - \mathbf{R}\hat{\mathbf{R}}^T\|$. Signature: $T_1 \times T_2 \rightarrow \mathbb{R}^+ \in [0, 2\sqrt{2}]$.

ACKNOWLEDGMENT

We would like to thank our colleagues Samuele Tosatto, Erwan Renaudo and Hector Villeda for their helpful comments towards improving this paper.

REFERENCES

- [1] Urdf/XML/joint - ROS Wiki. [Online]. Available: <http://wiki.ros.org/urdf/XML/joint>
- [2] M. Abadi, P. Barham, J. Chen, Z. Chen, A. Davis, J. Dean, M. Devin, S. Ghemawat, G. Irving, M. Isard, M. Kudlur, J. Levenberg, R. Monga, S. Moore, D. G. Murray, B. Steiner, P. Tucker, V. Vasudevan, P. Warden, M. Wicke, Y. Yu, and X. Zheng, "TensorFlow: A system for large-scale machine learning," in *12th USENIX Symposium on Operating Systems Design and Implementation (OSDI 16)*, pp. 265–283. [Online]. Available: <http://www.usenix.org/system/files/conference/osdi16/osdi16-abadi.pdf>
- [3] B. M. Bell, "C++pad: a package for c++ algorithmic differentiation," *Computational Infrastructure for Operations Research*, vol. 57, no. 10, 2012.

- [4] J. Bradbury, R. Frostig, P. Hawkins, M. J. Johnson, C. Leary, D. Maclaurin, G. Necula, A. Paszke, J. VanderPlas, S. Wanderman-Milne, and Q. Zhang, "JAX: Composable transformations of Python+NumPy programs." [Online]. Available: <http://github.com/google/jax>
- [5] J. Carpentier, G. Saurel, G. Buondonno, J. Mirabel, F. Lamiroux, O. Stasse, and N. Mansard, "The Pinocchio C++ library : A fast and flexible implementation of rigid body dynamics algorithms and their analytical derivatives," in *2019 IEEE/SICE International Symposium on System Integration (SII)*, pp. 614–619.
- [6] D. Coleman, I. Sucas, S. Chitta, and N. Correll, "Reducing the Barrier to Entry of Complex Robotic Software: A MoveIt! Case Study," *arXiv:1404.3785 [cs]*, Apr. 2014, <http://arxiv.org/abs/1404.3785>.
- [7] A.-V. Duka, "Neural Network based Inverse Kinematics Solution for Trajectory Tracking of a Robotic Arm," vol. 12, pp. 20–27. [Online]. Available: <https://linkinghub.elsevier.com/retrieve/pii/S2212017313006361>
- [8] F. Díaz Ledezma and S. Haddadin, "First-order-principles-based constructive network topologies: An application to robot inverse dynamics," in *2017 IEEE-RAS 17th International Conference on Humanoid Robotics (Humanoids)*, pp. 438–445.
- [9] C. D. Freeman, E. Frey, A. Raichuk, S. Girgin, I. Mordatch, and O. Bachem, "Brax - a differentiable physics engine for large scale rigid body simulation." [Online]. Available: <http://github.com/google/brax>
- [10] M. Görner, R. Haschke, H. Ritter, and J. Zhang, *MoveIt! Task Constructor for Task-Level Motion Planning*, May 2019.
- [11] E. Heiden, D. Millard, E. Coumans, Y. Sheng, and G. S. Sukhatme, "NeuralSim: Augmenting differentiable simulators with neural networks," in *Proceedings of the IEEE International Conference on Robotics and Automation (ICRA)*. [Online]. Available: <https://github.com/google-research/tiny-differentiable-simulator>
- [12] I. Herzig, "Hrl-kdl." [Online]. Available: <https://github.com/herzig/hrl-kdl>
- [13] D. Q. Huynh, "Metrics for 3D Rotations: Comparison and Analysis," vol. 35, no. 2, pp. 155–164. [Online]. Available: <http://link.springer.com/10.1007/s10851-009-0161-2>
- [14] S. James, A. J. Davison, and E. Johns, "Transferring End-to-End Visuomotor Control from Simulation to Real World for a Multi-Stage Task." [Online]. Available: <http://arxiv.org/abs/1707.02267>
- [15] R. Köker, C. Öz, T. Çakar, and H. Ekiz, "A study of neural network based inverse kinematics solution for a three-joint robot," vol. 49, no. 3, pp. 227–234. [Online]. Available: <https://www.sciencedirect.com/science/article/pii/S0921889004001666>
- [16] F. D. Ledezma and S. Haddadin, "FOP Networks for Learning Humanoid Body Schema and Dynamics," in *2018 IEEE-RAS 18th International Conference on Humanoid Robots (Humanoids)*, pp. 1–9.
- [17] F. Meier, A. Wang, G. Sutanto, Y. Lin, and P. Shah, "Differentiable and Learnable Robot Models." [Online]. Available: <http://arxiv.org/abs/2202.11217>
- [18] A. Paszke, S. Gross, F. Massa, A. Lerer, J. Bradbury, G. Chanan, T. Killeen, Z. Lin, N. Gimelshein, L. Antiga, A. Desmaison, A. Kopf, E. Yang, Z. DeVito, M. Raison, A. Tejani, S. Chilamkurthy, B. Steiner, L. Fang, J. Bai, and S. Chintala, "Pytorch: An imperative style, high-performance deep learning library," in *Advances in Neural Information Processing Systems 32*, H. Wallach, H. Larochelle, A. Beygelzimer, F. d'Alch'e-Buc, E. Fox, and R. Garnett, Eds. Curran Associates, Inc., 2019, pp. 8024–8035. [Online]. Available: <http://papers.neurips.cc/paper/9015-pytorch-an-imperative-style-high-performance-deep-learning-library.pdf>
- [19] M. Quigley, B. Gerkey, K. Conley, J. Faust, T. Foote, J. Leibs, E. Berger, R. Wheeler, and A. Ng, "ROS: An open-source Robot Operating System," p. 6.
- [20] N. Vahrenkamp, M. Wächter, M. Kröhnert, K. Welke, and T. Asfour, "The robot software framework armarx," *it-Information Technology*, vol. 57, no. 2, pp. 99–111, 2015.
- [21] R. Villegas, J. Yang, D. Ceylan, and H. Lee, "Neural kinematic networks for unsupervised motion retargeting," in *Proceedings of the IEEE Conference on Computer Vision and Pattern Recognition (CVPR)*, June 2018.
- [22] X. Zhou, X. Sun, W. Zhang, S. Liang, and Y. Wei, "Deep kinematic pose regression," in *European Conference on Computer Vision*. Springer, pp. 186–201.